

# Effects of spin current on ferromagnets

Z. Li, J. He and S. Zhang

*Department of Physics and Astronomy, University of Missouri-Columbia, Columbia, MO 65211*

(Dated: November 5, 2018)

When a spin-polarized current flows through a ferromagnet, the local magnetization receives a spin torque. Two consequences of this spin torque are studied. First, the uniformly magnetized ferromagnet becomes unstable if a sufficiently large current is applied. The characteristics of the instability include spin wave generation and magnetization chaos. Second, the spin torque has profound effects on the structure and dynamics of the magnetic domain wall. A detail analysis on the domain wall mass, kinetic energy and wall depinning threshold is given.

PACS numbers: 75.75.+a, 75.30.Ds, 75.60.Ch, 72.25.Ba

## I. INTRODUCTION

There are many interesting phenomena generated by electronic current. In this paper, we focus our discussions on two effects: domain wall dynamics and magnetization instability. Recently, both topics have received considerably interests in experiments [1, 2, 3, 4, 5, 6, 7, 8, 9, 10, 11] and in theories [12, 13, 14, 15, 16, 17, 18, 19]. It is shown that the current is able to displace magnetic domain walls in a spin valve [3], in a constricted nanowire [4], in U-shaped (or L-shaped) nanowires [5, 6], in a ring structure [7] and in zigzag wires [8]. The current also generates dynamic domain walls (time-dependent wall structure) via the generation of spin waves in the uniformly magnetized ferromagnet. The point-contact experiments on a single layer ferromagnet [9, 10, 11] are likely associated with the interface spin waves excitations [12].

The physics of these experimental results is believed to be the consequence of spin angular momentum transfer, originally proposed by Slonczewski [22] and Berger [23] in magnetic multilayers. The extension of Slonczewski's model to a homogeneous ferromagnet has been carried out by several groups [14, 15, 16, 17]. Recently, we introduce two spin torques in ferromagnets [18]. With our spin torque model, most of the experimental observations can be quantitatively analyzed. This paper is organized as follows. In Sec. II, we briefly review the mechanism of the spin torque in a single ferromagnet. In Sec. III, we study the bulk and surface spin waves by applying the spin torque model. Several key characteristics of the magnetization instability driven by spin torques are predicted. In Sec. IV, we analyze the domain wall dynamics with and without defects. We also construct an analytic 1-D model to help understanding the key features in simulations. Finally, an outlook for the effects of spin torques in ferromagnets is presented in Sec. V.

## II. MECHANISM OF SPIN TORQUES IN FERROMAGNETS

The spin-polarized current does not interact with spatially uniform magnetization, except the classical Zeeman coupling between the current-induced magnetic field and

the magnetization. In a real ferromagnet, the magnetization is not spatially uniform due to the presence of various magnetic interactions, which tend to break the ferromagnet into domains. Even in a small particle, where the single domain assumption is approximately valid, the thermal fluctuation leads to a time-dependent non-uniform magnetization. In response to the spatially non-uniform magnetization, the spin current will be position-dependent and the spatial varying spin current produces the mechanism of the spin angular momentum transfer. To determine the spin transfer torque, one requires simultaneously solving the magnetization dynamics and the time-dependent spin current, which would be a very complex problem. Fortunately, the dynamics of the magnetization is much slower than that of the transporting electrons, then it is a good approximation to work on the transport equation with magnetization "frozen" spatially and temporally. Similar to the calculation of electron dynamics in an atom: the electronic structure is calculated by freezing the dynamics of nuclei.

Most of the theories of spin torques are built on the above approximation. Additional assumptions are needed to derive analytical expressions of the spin torque. Berger [23] first investigated the current-induced domain wall motion and introduced the "domain drag force" by using an intuitively physics picture that the current can drag the domain wall moving along the path of the current flow via an *s-d* exchange interaction. Since the spin torque was not mathematically formulated in this work, it is unclear how to solve the problem of domain wall dynamics for a realistic magnetic wire by using this intuitive approach. Bazaliy *et al* [15] proposed a spin torque model in a ferromagnet within the ballistic transport model for half-metallic materials and they found that the spin torque is  $\tau \propto (\mathbf{j}_e \cdot \nabla \mathbf{M})$  where  $\mathbf{j}_e$  is the electric current. The essential assumption is that the spin polarization of the current is parallel to the local magnetization, i.e., an adiabatic approximation. The above explicit expression of the spin torque can be immediately combined with the well-known LLG equation to calculate the response of magnetization to the spin torque. Waintal and Viret [16] has extended this approximation by relaxing the adiabatic approximation. They have shown that the spin polarization of the current is not parallel

to the local magnetization in a ballistic transport model. However, no clear mathematical expression is given to implement this additional spin torque to the LLG equation. Tatara and Kohno [17] proposed two spin current effects: an adiabatic torque mentioned above and a momentum transfer torque. The momentum transfer effect originates from the momentum scattering by a domain wall and it is proportional to wall resistivity. This momentum transfer effect is negligible except for very thin walls.

We have proposed the spin torque by evaluating the response of the conduction electron spins in a spatially and temporally varying magnetization  $\mathbf{M}(\mathbf{r}, t)$  in the semi-classical transport theory [18]. The spin torque has been formulated in the following form

$$\tau_s = b_J(\hat{\mathbf{j}}_e \cdot \nabla)\mathbf{M} - \frac{c_J}{M_s}\mathbf{M} \times (\hat{\mathbf{j}}_e \cdot \nabla)\mathbf{M} \quad (1)$$

where  $\hat{\mathbf{j}}_e$  is the unit vector in the direction of the current flow,  $b_J = Pj_e\mu_B/eM_s$ ,  $P$  is the spin polarization of the current,  $M_s$  is the saturation magnetization,  $\mu_B$  is Bohr magneton,  $c_J = \zeta b_J$ , and  $\zeta$  is a dimensionless constant that describing the degree of the nonadiabaticity between the spin of conduction electrons and the local magnetization. For a typical ferromagnet (Ni, Co, Fe and their alloys),  $\zeta$  is within a range of 0.001  $\sim$  0.05. The physical interpretation is that the  $b_J$  term is an adiabatic spin torque, describing the adiabatic process of the non-equilibrium conduction electrons, i.e., the direction of the spin polarization of current is parallel to the local magnetization within a domain wall; the  $c_J$  term is a non-adiabatic torque, which is related to the spatial mis-tracking of spins between conduction electrons and local magnetization.

The advantage of expressing the spin torques in the form Eq. (1) is that one can readily generalize LLG equation in the presence of the spin current,

$$\frac{\partial \mathbf{M}}{\partial t} = -\gamma \mathbf{M} \times \mathbf{H}_{eff} + \frac{\alpha}{M_s} \mathbf{M} \times \frac{\partial \mathbf{M}}{\partial t} + \tau_s \quad (2)$$

where  $\gamma$  is the gyromagnetic ratio, and  $\mathbf{H}_{eff}$  is the effective magnetic field including the external field, the anisotropy field, magnetostatic field, and the exchange field, and  $\alpha$  is the Gilbert damping parameter. The current-driven magnetization dynamics will be studied by solving this generalized LLG equation in various situations.

### III. SPIN WAVE EXCITATIONS

In this section, we apply our generalized LLG equation, Eq. (2) to study the spin wave excitations in a single layer magnetic film. The local effective field is

$$\mathbf{H}_{eff} = \frac{H_K M_x}{M_s} \mathbf{e}_x + \frac{2A}{M_s^2} \nabla^2 \mathbf{M} - 4\pi M_z \mathbf{e}_z + H_e \mathbf{e}_x \quad (3)$$

where  $H_K$  is the anisotropy field, along the  $x$ -axis,  $A$  is the exchange constant, and we include a self-demagnetization field  $4\pi M_z$  of the film. The initial magnetization saturates in the direction of the magnetic field  $H_e$  along the  $x$ -axis in the plane of the layer.

When one applies a sufficiently large current along the  $x$ -axis, the uniformly magnetized film becomes unstable. To see this, we consider a small deviation of the magnetization vector from the easy axis  $\mathbf{e}_x$ ,

$$\mathbf{M} = M_s \mathbf{e}_x + \delta \mathbf{m} e^{i(\omega t + \mathbf{k} \cdot \mathbf{r})} \quad (4)$$

where  $\delta \mathbf{m}$  is a small vector. Inserting Eqs. (3) and (4) into Eq. (2), and keeping only the terms linear in  $\delta \mathbf{m}$ , we obtain two linearized equations for  $\delta m_y$  and  $\delta m_z$ . A secular equation is then established for the spin wave frequency  $\omega$  and the spin wavevector  $\mathbf{k}$ .

$$\begin{bmatrix} -i(\omega - b_J k_x) & A_1 \\ A_2 & -i(\omega - b_J k_x) \end{bmatrix} \begin{bmatrix} \delta m_y \\ \delta m_z \end{bmatrix} = 0 \quad (5)$$

where we have defined  $A_1 = -\gamma \left( \frac{2A}{M_s} k^2 + 4\pi M_s + H \right) - i\alpha\omega + ic_J k_x$  and  $A_2 = \gamma \left( \frac{2A}{M_s} k^2 + H \right) + i\alpha\omega - ic_J k_x$ , in which  $k^2 = k_x^2 + k_y^2 + k_z^2$  and  $H = H_e + H_K$ .

The above linearized equations have a non-zero solution if and only if

$$\det \begin{bmatrix} -i(\omega - b_J k_x) & A_1 \\ A_2 & -i(\omega - b_J k_x) \end{bmatrix} = 0 \quad (6)$$

The above equation establishes the relation between the spin wave frequency  $\omega$  and the wavevector  $\mathbf{k}$ . For a real wavevector  $\mathbf{k}$ ,  $\omega$  is a complex number. If the imaginary part of  $\omega$  becomes negative, Eq. (4) is exponentially growing with time. In this case, the uniform magnetization becomes unstable. One may define the critical current such that  $Im \omega = 0$ . From Eq. (6), we find  $Re \omega = c_J k_x / \alpha$  and

$$\frac{\gamma}{k_x} \sqrt{\left( \frac{2A}{M_s} k^2 + H \right) \left( \frac{2A}{M_s} k^2 + H + 4\pi M_s \right)} b_J - c_J / \alpha = 0 \quad (7)$$

Equations (7) gives out the current density required to generate spin waves with a given wave vector  $\mathbf{k}$ . Interestingly, the minimum current density does not occur at the uniform mode of  $\mathbf{k} = 0$  as in the ordinary spin wave excitations, rather the spin wave with a finite wavevector is first excited by the current. To see this, we minimize  $b_J - c_J / \alpha$  in Eq. (7) with respect to the wavevector, and we find the minimum current density occurs at

$$k_x^2 = \frac{M_s}{2A} \sqrt{(4\pi M_s + H)H}. \quad (8)$$

and  $k_y = k_z = 0$ . The corresponding wavelength is,

$$\lambda_c = \frac{1}{k_x} = \sqrt{\frac{2A}{M_s}} [(4\pi M_s + H)H]^{-1/4}. \quad (9)$$

The new length scale given above places a severe limitation on micromagnetics: one needs to choose mesh size to be smaller than  $\lambda_c$  when the current density exceeds the critical current density, in order to correctly capture the current-driven effects in the simulation. For certain parameters, particularly at large magnetic fields,  $\lambda_c$  can be comparable or smaller than the exchange length.

Inserting Eq. (8) back to Eq. (7), we find that the minimum current density for the instability is,

$$|b_J - c_J/\alpha|_{min} = \gamma \sqrt{\frac{2A}{M_s}} \left( \sqrt{H} + \sqrt{H + 4\pi M_s} \right). \quad (10)$$

Note that we have assumed a spin wave spectrum in the form of Eq. (8) which represents a spin wave in an isotropic infinite medium. If we take  $\zeta = \alpha$  the spin wave instability does not occur for any large spin currents.

In experiments, the current may not uniform across the sample. For example, the current density is very large at the contact area in the point-contact experiments and it becomes negligibly small away from the contact area. In this case, the excited spin waves are confined in a narrow region near the interface. To access the spin wave instability in this situation, we consider a surface spin wave mode

$$\mathbf{M} = M_s \mathbf{e}_x + \delta \mathbf{m} e^{-x/\kappa} e^{i(\omega t + k_y y + k_z z)}. \quad (11)$$

where  $\kappa$  is the penetration length.

By inserting it into Eq. (2) and by repeating the derivation similarly, we find the instability  $Im \omega = 0$  occurs at

$$-(b_J + \alpha c_J) = \gamma \alpha \kappa \left( \frac{2A}{M_s} (k_y^2 + k_z^2) + H + 2\pi M_s \right). \quad (12)$$

Note a negative sign on the left-hand side; it indicates that the surface spin waves can only be generated by the current flowing along one direction. This result is consistent with the point-contacted experiments [10], in which the current flowing from the magnetic layer to the non-magnetic tip is able to excite spin waves. The magnitude of the critical current for surface spin wave is proportional to the damping parameter  $\alpha$  and the penetration length  $\kappa$ . We note that the exchange field at the surface for the localized spin wave is  $(2Aa_0/M_s^2)\nabla_x \mathbf{M}$  where  $a_0$  is the lattice constant so that the exchange field inside the layer  $(2A/M_s^2)\nabla_x^2 \mathbf{M}$  will be compensated. This is the reason that the right hand side of Eq. (12) does not contain the  $k_x^2$  term.

An estimation on the magnitude of spin wave instability can be readily done by using the materials parameters of Co:  $\gamma = 1.9 \times 10^7 (Oe)^{-1} s^{-1}$ ,  $4\pi M_s = 1.8 \times 10^4 Oe$ ,  $H_K = 500 Oe$ ,  $M_s = 14.46 \times 10^5 A/m$ ,  $A = 2.0 \times 10^{-11} J/m$  and  $P = 0.35$ . If one takes the damping parameter to be 0.01, the non-adiabaticity  $\zeta = 0.02$ , the penetration length of 5 nm, and  $k_y = k_z \approx 0$  for the long wave length limit, we find that the critical current at  $H_e = 0 Oe$  is  $j_{min}^{bulk} = 1.12 \times 10^{10} A/cm^2$  for the bulk

spin wave and  $j_{min}^{surface} = 6.4 \times 10^7 A/cm^2$  for the surface mode, which is two orders of magnitude smaller than that of bulk spin wave.

The fact that the large enough current density can excite spin waves with different wave lengths raises a question: what is the magnetization state at the large current density? Shibata *et al* [19] predicted that a *static* multi-domain state can be formed if the current exceeds a second critical current higher than the critical current density defined above. By using Eq. (16), we find that the *static* domain configuration is unlikely to form. This is because the domain will be moving with an average velocity determined by the non-adiabatic torque  $c_J/\alpha$  [18, 20] seen in next section. We had reported earlier that a large current density drives the uniform magnetization into spatially and temporally chaotic motion [21]. The detail analysis on this transition will be given elsewhere.

#### IV. DOMAIN WALL MOTION

One of the most interesting predictions on the domain wall motion is that a steady domain wall velocity is independent of  $b_J$ . Rather the steady state velocity is solely determined by the non-adiabatic torque and the external magnetic field. We show the proof below.

In a steady state motion, one can assume the magnetization vector  $\mathbf{M} = \mathbf{M}(x - v_x t, y, z)$ . Then,  $\partial \mathbf{M} / \partial t = -v_x \partial \mathbf{M} / \partial x$ . For a current applied in x-axis, the LLG equation, Eq. (2), is thus

$$(b_J + v_x) \frac{\partial \mathbf{M}}{\partial x} - \frac{\alpha v_x + c_J}{M_s} \mathbf{M} \times \frac{\partial \mathbf{M}}{\partial x} = \gamma \mathbf{M} \times \mathbf{H}_{eff} \quad (13)$$

By performing inner-product of  $\mathbf{M} \times \partial \mathbf{M} / \partial x$  with the above equation, one has

$$\frac{\alpha v_x + c_J}{M_s} \left| \mathbf{M} \times \frac{\partial \mathbf{M}}{\partial x} \right|^2 = \gamma \mathbf{H}_{eff} \cdot \frac{\partial \mathbf{M}}{\partial x} \quad (14)$$

We now integrate the above equation over the entire domain wall. We find

$$\frac{\alpha v_x + c_J}{\gamma M_s} \int dV \left| \frac{\partial \mathbf{M}}{\partial x} \right|^2 = \int dV \frac{\partial E}{\partial x} = \frac{1}{v_x} \frac{\partial}{\partial t} \int E dV \quad (15)$$

where  $E$  is the energy density that is defined  $dE = -\mathbf{H}_{eff} \cdot d\mathbf{M}$ , and we have also used the fact that  $\mathbf{M}$  and  $\partial \mathbf{M} / \partial x$  is perpendicular. The right-hand side of the equation becomes  $\pm 2S_0 M_s H_e$  because the rate of the total energy change for a uniformly moving wall is  $2S_0 M_s H_e v_x$ , where  $S_0$  is the cross section perpendicular to the moving wall. Therefore, the velocity is

$$v_x = -\frac{c_J}{\alpha} \pm \frac{\gamma H_e W}{\alpha} \quad (16)$$

where we have defined the wall width  $W$

$$W^{-1} = \frac{1}{2S_0 M_s^2} \int dV \left| \frac{\partial \mathbf{M}}{\partial x} \right|^2 \quad (17)$$

The striking conclusion from Eq. (16) is that the wall velocity in the absence of the magnetic field is exactly  $-c_J/\alpha$  for any type of walls as long as the wall is moving at a constant velocity. Without the current, Eq. (16) becomes the well-known Walker's velocity [24]. We should point out that the wall width, Eq. (17), is weakly dependent on the magnetic field and the adiabatic torque  $b_J$  [14], and thus the terminal wall velocity will slightly depend on  $b_J$  in the presence of the field.

The wall velocity given by Eq. (16) breaks down when the wall is *not* moving with a constant velocity. To describe a non-uniform wall motion, it is necessary to postulate an approximate wall structure. Here, we follow Walker's procedure [24] by introducing two polar angles  $\theta$  and  $\varphi$  in the form mimic a transverse domain wall [25]. By placing the explicit form of  $\theta$  into Eq. (2), we find

$$\frac{d\varphi}{dt} = \gamma(H_e - 4\pi\alpha M_s \sin\varphi \cos\varphi) + \frac{\alpha b_J - c_J}{W} \quad (18)$$

$$\alpha v_x(t) + W \frac{d\varphi}{dt} = \gamma H_e W - c_J \quad (19)$$

where  $\varphi$  is the out-of-plane angle of the magnetization vector,  $v_x(t)$  is the velocity, and we have discarded  $\alpha^2$  terms.

To further gain insights of the wall velocity, we assume that the distortion of the wall is small during the wall motion. Then, we treat the wall width  $W$  as time-independent constant, and replace  $\sin\varphi \cos\varphi$  by  $\varphi$  in Eq. (18). By differentiating Eqs. (18) and (19) with respect to  $t$ , and by eliminating  $\varphi$  in the resulting equations, we find the equation for the wall velocity

$$m^* \frac{dv_x(t)}{dt} + \frac{2M_s\alpha}{\gamma W} v_x(t) - 2M_s H_e + \frac{2M_s}{\gamma W} c_J = 0 \quad (20)$$

where we have defined the domain wall effective mass per unit area as [26],

$$m^* = (2\pi\gamma^2 W)^{-1}. \quad (21)$$

Equation (20) reveals that the domain wall can be treated as a particle with an effective mass  $m^*$ , subjecting to a friction force (second term) and external forces from the magnetic field (third term) and the current (fourth term). Interestingly, the adiabatic torque does not contribute to the current-driving force. The solution of Eq. (20) is

$$v_x(t) = -\frac{c_J - \gamma W H_e}{\alpha} + C e^{-t/\tau} \quad (22)$$

where  $\tau = (4\pi M_s \gamma \alpha)^{-1}$  is the relaxation time and  $C$  is a constant determined by the initial condition. If one assumes that the field or the current is applied at  $t = 0$ , i.e.,  $\varphi(0) = 0$ , we find, from Eq. (18) and (19),  $v_x(0) = -b_J$ . By using this initial value of the velocity, Eq. (22) becomes

$$v_x(t) = -\frac{c_J - \gamma W H_e}{\alpha} \left(1 - e^{-t/\tau}\right) - b_J e^{-t/\tau} \quad (23)$$

One may understand the above two terms as follows. The first is a "translational" velocity and one might introduce a kinetic energy

$$E = \frac{1}{2} m^* v_x^2(t) = \frac{(c_J - \gamma W H_e)^2}{4\pi\gamma^2 W \alpha^2} \left(1 - e^{-t/\tau}\right)^2 \quad (24)$$

The time scale to establish a fully accelerated motion is determined by  $\tau$ . For a Co wire,  $\tau = 0.3$  ns if we take  $\alpha = 0.01$ . The second term of the Eq. (23) is related to the domain wall distortion, and therefore, it does not contribute the mobility of the domain wall. The displacement of the domain wall is  $x_c = \int_0^\tau v_x(t) dt$ .

We illustrate below that the concept of the "translational" kinetic energy is helpful in understanding the domain wall motion in a nanowire containing defects or pinning centers. For example, let us consider a domain wall propagation from one place (A) to another place (B), shown in Fig. 1(a). Between A and B regions, there is a distribution of defects. We show that the minimum current-density or the minimum magnetic field required to overcome these pinning centers depends on the relative distance between the defects and the domain wall. If a strong defect is located far away from the initial domain wall position (A), the domain wall is able to develop its fully kinetic energy, and the domain wall is able to pass through the pinning center when the kinetic energy is larger than pinning potential. On the other hand, if the defect locates near the initial wall center, the kinetic energy is small when the domain wall encounters the defect and thus a relative weak defect potential is able to trap the domain wall. To be more quantitative, we perform the following calculation.

We model a defect by introducing an artificial local anisotropy pinning source in an otherwise perfect nanowire. The anisotropy of the defect is  $H_d = 4H_K$  which is 4 times larger than the anisotropy of the wire,  $H_K = 500$  Oe. We choose a one-dimensional model, i.e., the magnetization does not vary in the direction of width and thickness, to illustrate our points. The easy axis of the wire and the defect, and the current or magnetic field, are all along x-axis. The mesh size in x-direction is 4 nm. Before one turns on the current, a stationary Néel wall is centered at  $x = 0$ , and the defect is located  $x_d$  from the center of the wall. At  $t = 0$ , a current is turned on and we calculate the domain wall motion afterwards.

First, we have placed the defect far away from the region A, i.e.,  $x_d \gg \int_0^\tau v_x(t) dt$ , we find that the critical current is proportional to the damping parameter in the absence of magnetic field, consistent with Eq. (24). When we vary the exchange constant which effectively changes the domain wall width, we find that the critical current scales as  $\sqrt{W}$ , again, consistent with Eq. (24). We now vary the defect position. In Fig. 1(b), we show the critical current as a function of the defect position. As expected, the critical current decreases as one places the defect away from the original wall. The initial increase of the critical current at small distance comes from the adiabatic torque,  $b_J$ . When the defect is very near the

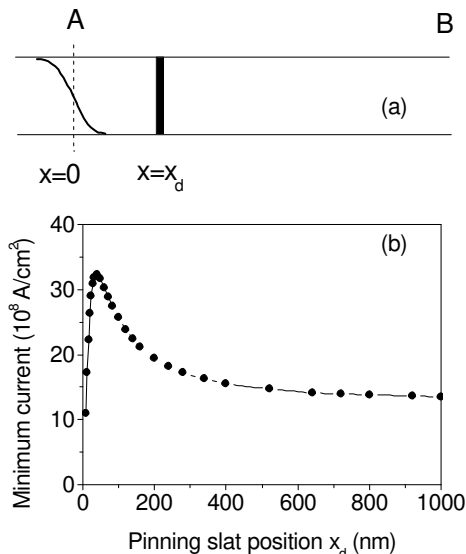


FIG. 1: (a) Schematic pinning source in a Co nanowire, (b) The minimum spin current required for a wall propagation through a pinning as a function of pinning position  $x_d$ . The parameters of Co are  $4\pi M_s = 1.8 \times 10^4$  Oe,  $H_K = 500$  Oe,  $M_s = 14.46 \times 10^5$  A/m,  $A = 2.0 \times 10^{-11}$  J/m,  $H_e = 0$ ,  $\zeta = 0.02$  and  $\alpha = 0.006$

original wall, the displacement of the wall by the  $b_J$  term exceeds  $x_d$  and thus the wall overcomes the defect potential by the adiabatic torque. Therefore, at the small distance, the adiabatic torque is more effective than the kinetic energy involved.

## V. OUTLOOK

There are many fundamental issues on current-induced effects. We intend to list a few of them below.

On the fundamental mechanism, the spin torque given by Eq. (1) is valid up to the first derivative in space.

When the domain wall thickness is extremely small in some nanoconstriction, the high order terms become important. A better quantum mechanical treatment for the spin torque is required to re-formulate the spin torque in this case.

In a large field or a large current, the wall is usually moving quite irregularly. Non-uniform wall motion appears: the wall can be bounced back and forth in transverse directions, and the wall changes its structure. For example, the current can drive vortex wall motion relatively easier than the transverse wall in the presence of defects. However, the vortex wall is usually unstable during its motion and the vortex wall tends to change into a transverse wall. These detailed complications have to be studied via numerical solutions of the LLG equation [20, 27]. To model a realistic device, an extensive numerical effort is required.

The effect of Joule heating by the current has not been quantified. The experimental results show that the sample temperature increases less than 5 K when the current density is order of  $10^5 \sim 10^6$  A/cm<sup>2</sup> [3], while the temperature is dramatically increased when the current density is  $10^7$  A/cm<sup>2</sup> [28]. These studies are for a steady current density. In most of the devices, it is much desirable to use a pulsed current source. A thorough study on the Joule heating on the amplitude and duration of the current seems very important. Frequently, the observed critical current is smaller than the optimal theoretical value by a factor of two. Whether it is due to heating is unclear at the present time.

The finite temperature theory on the domain wall motion is lacking. It would be interesting to study the lifetime of a trapped domain wall and it takes for the current to depinning the wall at finite temperature. Similar to the effect of the finite temperature in current-driven switching in spin valves, we expect that the role of temperature has profound effects on domain wall motion.

The research was supported by NSF (ECS-0223568 and DMR-0314456).

- 
- [1] L. Gan, S. H. Chung, K. H. Aschenbach, M. Dreyer and R. D. Gomez, IEEE Trans. Magn. bf 36, 3047 (2000).
  - [2] H. Koo, C. Krafft, and R. D. Gomez, Appl. Phys. Lett. **81**, 862 (2002).
  - [3] J. Grollier, P. Boulenc, V. Cros, A. Hamzić, A. Vaurés, A. Fert and G. Faini, Appl. Phys. Lett. **83**, 509 (2003).
  - [4] M. Tsoi, R. E. Fontana, S. S. P. Parkin, Appl. Phys. Lett. **83**, 2261 (2003).
  - [5] N. Vernier, D. A. Allwood, D. Atkinson, M. D. Cooke and R. P. Cowburn, Europhys. Lett. **65**, 526 (2004).
  - [6] A. Yamaguchi, T. Ono, S. Nasu, K. Miyake, K. Mibu, and T. Shinjo Phys. Rev. Lett. **92**, 077205 (2004).
  - [7] M. Kläui, C. A. F. Vaz, J. A. C. Bland, W. Wernsdorfer, G. Faini, E. Cambril, L. J. Heyderman, F. Nolting, and U. Rüdiger, Phys. Rev. Lett. **94**, 106601 (2005).
  - [8] M. Kläui, P.-O. Jubert, R. Allenspach, A. Bischof, J. A. C. Bland, G. Faini, U. Rüdiger, C. A. F. Vaz, L. Vila, and C. Vouille, Phys. Rev. Lett. **95**, 026601 (2005).
  - [9] M. Tsoi, V. Tsoi, J. Bass, A. G. M. Jansen, and P. Wyder, Phys. Rev. Lett. **89**, 246803 (2002).
  - [10] Y. Ji, C. L. Chien, and M. D. Stiles, Phys. Rev. Lett. **90**, 106601 (2003); T. Y. Chen, Y. Ji, C. L. Chien and M. D. Stiles, Phys. Rev. Lett. **93**, 026601 (2004).
  - [11] B. Özyilmaz, A. D. Kent, J. Z. Sun, M. J. Rooks, and R. H. Koch, Phys. Rev. Lett. **93**, 176604 (2004)
  - [12] Z. Li and S. Zhang, Phys. Rev. Lett. **92**, 207203 (2004).
  - [13] M. D. Stiles, J. Xiao, and A. Zangwill, Phys. Rev. B **69**, 054408 (2004).
  - [14] Z. Li and S. Zhang, Phys. Rev. B **70**, 024417 (2004).
  - [15] Ya. B. Bazaliy, B. A. Jones, and S.-C. Zhang, Phys. Rev. B **57**, R3213 (1998).
  - [16] X. Waintal and M. Viret, Europhy. Lett. **65**, 427 (2004).

- [17] G. Tatara and H. Kohn, Phys. Rev. Lett. **92**, 086601 (2004).
- [18] S. Zhang and Z. Li, Phys. Rev. Lett. **93**, 127204 (2004).
- [19] J. Shibata, G. Tatara and H. Kohno, Phys. Rev. Lett. **94**, 076601 (2005).
- [20] A. Thiaville, Y. Nakatani, J. Miltat and Y Suzuki, Europhys. Lett. **69**, 990 (2005).
- [21] Z. Li, J. He, and S. Zhang, J. Appl. Phys. **97**, 10C703 (2005).
- [22] J. Slonczewski, J. Magn. Magn. Mater. **159**, L1 (1996); **195**, L261 (1999).
- [23] L. Berger, J. Appl. Phys. **49**, 2156 (1978); **55**, 1954 (1984).
- [24] N. L. Schryer and L. R. Walker, J. Appl. Phys. **45**, 5406 (1974).
- [25] By introducing a Walker's trial function,  $\varphi = \varphi(t)$ ;  $\ln \tan \frac{\theta}{2} = \frac{1}{W} \left( x - \int_0^t v_x(\tau) d\tau \right)$ , we can get the ordinary first-order differential equations to determine the wall width  $W$ , the angle  $\varphi(t)$  and the transient velocity  $v_x(t)$ , where  $\theta$  is the angle between the magnetization vector and the  $+x$  axis and  $\varphi$  is the out-of-plane angle of the magnetization vector.
- [26] A. P. Malozemoff, J. C. Slonczewski, *Magnetic Domain Walls in Bubble Materials*, Academic Press, New York, 1979.
- [27] J. He, Z. Li and S. Zhang, (unpublished).
- [28] A. Yamaguchi, S. Nasu, H. Tanigawa, T. Ono, K. Miyake, K. Mibu and T. Shinjo, Appl. Phys. Lett. **86**, 012511 (2005).